Subspace-Based Imaging Using Only Power Measurements

Belal Korany, Saandeep Depatla, and Yasamin Mostofi
University of California Santa Barbara
Santa Barbara, CA, USA
Email: {belalkorany, saandeep, ymostofi}@ece.ucsb.edu

***Abstract*—In this paper, we are interested in the high-resolution imaging of an unknown area based on only power measurements of a small number of wireless transceivers located on one side of the unknown area. In order to do so, we propose a framework that achieves a polynomial order reduction in the number of antennas required for high-resolution imaging. More specifically, we show that by spacing the antennas at multiples of the wavelength and applying subspace-based analysis, we can image M targets using only $2M+1$ transmit/receive antennas (as compared to the state-of-the-art value of M^2+1 antennas). We then validate our framework using simulations in both noise-free and noisy environments.**

***Index Terms*—Super-resolution imaging, Time Reversal MUSIC, Rytov Model.**

I. Introduction

Several techniques have been proposed in the literature to image an unknown area using wireless measurements [1]–[4]. Among these, inverse scattering solutions are heavily utilized [1], [3]. However, they are generally characterized by high computational complexity. To reduce the complexity, other techniques, such as subspace-based methods, have been proposed [5], [6]. Due to their simplicity and high-resolution capability, the subspace-based methods are often preferred when the number of targets in the unknown area is small, as compared to the number of available wireless nodes. The traditional subspace-based methods require the knowledge of the magnitude and phase of the received signal to image the targets in the unknown area. However, most of the commercial off-the-shelf transceivers (such as WiFi cards) cannot stably measure the phase [7], thus limiting the applicability of the subspace-based methods.

Recently, subspace-based methods, such as Time Reversal MUltiple SIgnal Classification (TR-MUSIC), have been extended to power-only scenarios. In [6], for instance, a power-only TR-MUSIC algorithm is proposed. But it requires the number of wireless transceivers to be greater than the square of the number of targets, which is impractical in many cases. In [8], the phase of the received signal is estimated at the receiving antenna array from the received power measurements, and then used to image the unknown area using conventional TR-MUSIC. However, this method relies on controlling and adapting the phases of the transmitted signals, which is not practical in most commercial wireless devices.

This work is funded by NSF CCSS award #1611254.

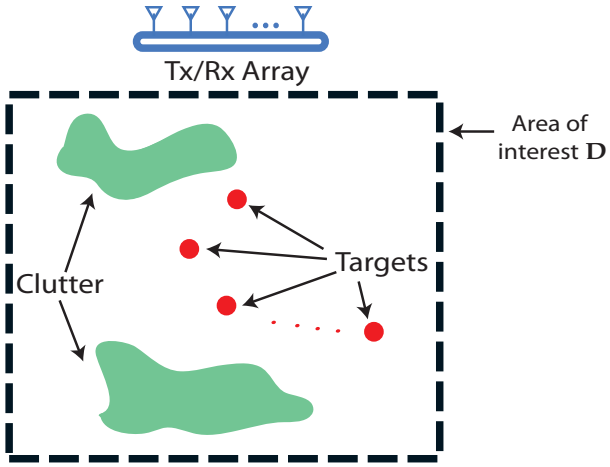

Fig. 1. An illustration of the considered scenario. The workspace $\mathbf{D}$ contains several targets of interest along with other objects. An array of transceivers are used for imaging. The Tx antennas transmit wireless signals that interact with the objects in $\mathbf{D}$ and are received by the Rx antennas. The goal of this paper is to image the targets in $\mathbf{D}$ using only the received power measurements of the Rx array.

In this paper, we are interested in imaging an unknown number of targets using only wireless power measurements, with an antenna array that is located on one side of the area (see Fig. 1), and with a small number of transceivers. We propose a framework to extend the TR-MUSIC algorithm to the case where only power measurements are available. More specifically, we show that by positioning the antennas multiple wavelengths apart, and extending TR-MUSIC to the resulting formulation, the number of the required wireless nodes has to only be greater than twice the number of the targets in the area (as compared to the square of the number of targets in [6]). Furthermore, we show that our method images the unknown area from only one side of the environment, which is of practical significance when not all the sides of the environment are accessible. Finally, our method does not require any manipulation of the phase of the transmitted signal at the transmitter side.

The rest of the paper is organized as follows. In Section II, we use the Rytov approximation to model the received power. In Section III, we present our framework to image the unknown area. We then validate our approach in Section IV with simulations. We conclude in Section V.

II. Problem Formulation

Consider a workspace $\mathbf{D}$ shown in Fig. 1. The workspace contains M targets of interest along with other objects, which we call the clutter. For instance, the workspace can be a building in which the targets of interest are humans, while the other objects, such as walls and furniture, form the clutter. An array of antennas located outside of the workspace $\mathbf{D}$ transmits wireless signals which interact with the objects in $\mathbf{D}$ and are then received back by the same array. Alternatively, two different antenna arrays (on the same side) can be used, one for transmission (Tx) and the other for reception (Rx). The goal of this paper is then to image the targets in the workspace using only the received power at the Rx antennas. In this section, we mathematically characterize the received power in terms of the targets in the workspace. To keep the formulation general and applicable to both cases of single and double arrays, we use a different notation to indicate the position of the Tx and Rx antennas.

Consider a Tx antenna located at $\mathbf{x}^t \in \mathbf{D}^{\text{out}}$, where $\mathbf{D}^{\text{out}}$ is the compliment of $\mathbf{D}$, radiating wireless signals into $\mathbf{D}$, and let $\mathbf{x}^r \in \mathbf{D}^{\text{out}}$ denote the location of an Rx antenna. Under the assumption of single-polarized Rx antenna, the electric field at $\mathbf{x}^r$ due to a transmission from a Tx antenna at $\mathbf{x}^t$ is given by the following scalar volume integral equation [9]:

$$E(\mathbf{x}^r,\mathbf{x}^t) = E_{\text{inc}}(\mathbf{x}^r,\mathbf{x}^t) + \iiint\limits_{\mathbf{D}} G(\mathbf{x}^r,\mathbf{x}')\tau(\mathbf{x}')E(\mathbf{x}',\mathbf{x}^t)d\mathbf{x}', \quad (1)$$

where $E_{\text{inc}}(\mathbf{x}^r,\mathbf{x}^t)$ is the incident field at $\mathbf{x}^r$, which is the received field in the absence of objects, $\tau(\mathbf{x}') = \omega^2\mu_o(\epsilon(\mathbf{x}') - \epsilon_o)$ and $\epsilon(\mathbf{x}')$ are the scattering strength, and the permittivity of an object at $\mathbf{x}' \in \mathbf{D}$, respectively, ω is the angular frequency of the signal, and ϵ_o and μ_o are the permittivity and permeability of free space, respectively. $G(\mathbf{x}^r,\mathbf{x}')$ denotes the free space Green's function between the points $\mathbf{x}'$ and $\mathbf{x}^r$and is given by,

$$G(\mathbf{x}^r,\mathbf{x}') = \frac{e^{j\frac{2\pi}{\lambda}|\mathbf{x}^r-\mathbf{x}'|}}{4\pi|\mathbf{x}^r-\mathbf{x}'|}, \quad (2)$$

where λ is the wavelength. The electric field $E(\mathbf{x}',\mathbf{x}^t)$ inside the integral of Eq. (1) depends on $\tau(\mathbf{x}')$, making it non-linear in objects and computationally intense to solve [9]. In the literature, several linearizing approximations have been proposed to solve Eq. (1) more efficiently. In this paper, we use Rytov approximation which relates the received power linearly to the targets in $\mathbf{D}$ [1]. Under this approximation, the electric field can be modeled as follows:

$$E(\mathbf{x}^r,\mathbf{x}^t) \approx E_{\text{inc}}(\mathbf{x}^r,\mathbf{x}^t)e^{\frac{E_{\mathbf{D}}(\mathbf{x}^r,\mathbf{x}^t)}{E_{\text{inc}}(\mathbf{x}^r,\mathbf{x}^t)}}, \quad (3)$$

where $E_{\mathbf{D}}(\mathbf{x}^r,\mathbf{x}^t) = \iiint\limits_{\mathbf{D}} G(\mathbf{x}^r,\mathbf{x}')\tau(\mathbf{x}')E_{\text{inc}}(\mathbf{x}',\mathbf{x}^t)d\mathbf{x}'$.

In this paper, we take the incident field to be the free space electric field: $E_{\text{inc}}(\mathbf{x}',\mathbf{x}^t) = G(\mathbf{x}',\mathbf{x}^t)$. Then from Eq. (3), the received power is given by,

$$P(\mathbf{x}^r,\mathbf{x}^t) = P_{\text{inc}}(\mathbf{x}^r,\mathbf{x}^t) + 10\log_{10}(e^2)\Re\left\{\frac{E_{\mathbf{D}}(\mathbf{x}^r,\mathbf{x}^t)}{E_{\text{inc}}(\mathbf{x}^r,\mathbf{x}^t)}\right\},$$

where $P(\mathbf{x}^r,\mathbf{x}^t) = 10\log_{10}(|E(\mathbf{x}^r,\mathbf{x}^t)|^2)$, $P_{\text{inc}}(\mathbf{x}^r,\mathbf{x}^t) = 10\log_{10}(|E_{\text{inc}}(\mathbf{x}^r,\mathbf{x}^t)|^2)$, $\Re\{.\}$ denotes the real part of the argument, and $|.|$ denotes the magnitude of the argument. After removing the free-space component, we then have the following:

$$P_{\mathbf{D}}(\mathbf{x}^r,\mathbf{x}^t) = \frac{P(\mathbf{x}^r,\mathbf{x}^t) - P_{\text{inc}}(\mathbf{x}^r,\mathbf{x}^t)}{10\log_{10}(e^2)} = \Re\left\{\frac{E_{\mathbf{D}}(\mathbf{x}^r,\mathbf{x}^t)}{G(\mathbf{x}^r,\mathbf{x}^t)}\right\}. \quad (4)$$

Equation (4) models the received power in terms of the objects in $\mathbf{D}$.

III. TR-MUSIC based Imaging

In this section, we propose an algorithm based on TR-MUSIC [5] to image the targets in the workspace using only the received power measurements of the Rx array.

Let $\mathbf{x}_j^t, j \in \{1,2,\cdots,N_t\}$ and $\mathbf{x}_i^r, i \in \{1,2,\cdots,N_r\}$ denote the locations of the Tx and Rx antennas, respectively, where N_t and N_r denote the number of Tx and Rx antennas.[1] As mentioned earlier, the main bottleneck in imaging with power measurements of the array is that a prohibitive number of transceivers (i.e., more than square of the number of targets) is required. We next propose a special positioning of the antennas that, when combined with the Rytov modeling, can drastically reduce the number of required antennas. More specifically, we propose to position the Tx and Rx array in a way such that the distance between any antenna in the Tx array and each antenna in the Rx array is a multiple of the wavelength λ, i.e., $|\mathbf{x}_j^t - \mathbf{x}_i^r| = s\lambda$ for all i,j, where s is an integer. Note that such a placement is trivial if all the antennas are positioned on a straight line. By using such a configuration, the Green's function in the denominator of Eq. (4) becomes real. We then define p as follows, using Eq. (2) and (4)

$$p(\mathbf{x}_i^r,\mathbf{x}_j^t) = \frac{P_{\mathbf{D}}(\mathbf{x}_i^r,\mathbf{x}_j^t)}{4\pi|\mathbf{x}_i^r-\mathbf{x}_j^t|} = \Re\left\{E_{\mathbf{D}}(\mathbf{x}_i^r,\mathbf{x}_j^t)\right\} = \Re\left\{\iiint\limits_{\mathbf{D}} G(\mathbf{x}_i^r,\mathbf{x}')\tau(\mathbf{x}')E_{\text{inc}}(\mathbf{x}',\mathbf{x}_j^t)d\mathbf{x}'\right\}. \quad (5)$$

We next show that subspace-based analysis can be applied to this measured quantity, p, something that would not have been possible without the proposed antenna spacing.

Let the M targets of interest be located at $\mathbf{x}_m \in \mathbf{D}$ for $m \in \{1,\ldots,M\}$. Since the workspace contains both the targets and clutter, the scattering strength of an object in workspace can be expressed as follows: $\tau(\mathbf{x}') = \tau^{\text{tg}}(\mathbf{x}')$ if $\mathbf{x}' \in \mathbf{D}^{\text{tg}} \subset \mathbf{D}$ and $\tau(\mathbf{x}') = \tau^{\text{cl}}(\mathbf{x}')$ if $\mathbf{x}' \in \mathbf{D}^{\text{cl}} \subset \mathbf{D}$, where $\mathbf{D}^{\text{tg}}$ and $\mathbf{D}^{\text{cl}}$

[1] As mentioned earlier, we can have a single array for both the Tx and Rx antennas, as shown in Fig. 1.

denote the support of the targets and the clutter respectively. Furthermore, we assume that the dimensions of the targets are small, compared to the wavelength, and hence consider the targets as point objects. Therefore, $\tau^{\text{tg}}(\mathbf{x}') \approx \tau_m \delta(\mathbf{x}' - \mathbf{x}_m)$, where $\delta(.)$ is the Dirac-delta function, $\mathbf{x}_m$ is the location, and τ_m is the scattering strength of the m^{th} target. By substituting these values in Eq. (5), we get,

$$p(\mathbf{x}_i^r, \mathbf{x}_j^t) = p^{\text{tg}}(\mathbf{x}_i^r, \mathbf{x}_j^t) + p^{\text{cl}}(\mathbf{x}_i^r, \mathbf{x}_j^t), \tag{6}$$

where

$$p^{\text{tg}}(\mathbf{x}_i^r, \mathbf{x}_j^t) = \Re\left\{ \sum_{m=1}^{M} \tau_m G(\mathbf{x}_i^r, \mathbf{x}_m) G(\mathbf{x}_m, \mathbf{x}_j^t) \right\}. \tag{7}$$

p^{cl} can be similarly expressed in terms of the clutter. By making prior measurements when no targets are present, the impact of clutter can be measured and thus removed from Eq. (6). We next show how to apply subspace-based methods for imaging based on p^{tg}. By forming a matrix whose element in the i^{th} row and j^{th} column is $p^{\text{tg}}(\mathbf{x}_i^r, \mathbf{x}_j^t)$, we get the following $N_r \times N_t$ matrix,

$$\begin{aligned} P^{\text{tg}} &= \Re\left\{ \sum_{m=1}^{M} \tau_m \mathbf{g}_m^r \mathbf{g}_m^{t\ T} \right\} \\ &= \sum_{m=1}^{M} \left(\tau_{m_\Re} \mathbf{g}_{m_\Re}^r - \tau_{m_\Im} \mathbf{g}_{m_\Im}^r \right) \ \mathbf{g}_{m_\Re}^{t\ T} \\ &\quad - \sum_{m=1}^{M} \left(\tau_{m_\Re} \mathbf{g}_{m_\Im}^r + \tau_{m_\Im} \mathbf{g}_{m_\Re}^r \right) \ \mathbf{g}_{m_\Im}^{t\ T}, \end{aligned} \tag{8}$$

where $\mathbf{g}_m^t = [G(\mathbf{x}_m, \mathbf{x}_1^t), G(\mathbf{x}_m, \mathbf{x}_2^t), \ldots, G(\mathbf{x}_m, \mathbf{x}_{N_t}^t)]^T$ is an $N_t \times 1$ vector of Green's functions from all the Tx antennas to the m^{th} object's location, $\mathbf{g}_m^r = [G(\mathbf{x}_1^r, \mathbf{x}_m), G(\mathbf{x}_2^r, \mathbf{x}_m), \ldots, G(\mathbf{x}_{N_r}^r, \mathbf{x}_m)]^T$ is an $N_r \times 1$ Green's functions from the m^{th} object's location to all the Rx antennas, and $\{.\}_\Re$ and $\{.\}_\Im$ denote the real and imaginary parts of the argument, respectively. We next use the properties of the matrix P^{tg} to image the targets in $\mathbf{D}$. More specifically, we show how P^{tg} is in a form to which TR-MUSIC analysis [5] can be applied.

Let $P^{\text{tg}} = U \Sigma V^H$ denote the Singular Value Decomposition (SVD) of P^{tg}, where $U_{N_r \times N_r}$ and $V_{N_t \times N_t}$ have orthonormal columns. Assume that $\min(N_t, N_r) > 2M$. Since the matrix P^{tg} is the sum of $2M$ independent matrices of rank 1 as evident from Eq. (8), the matrix P^{tg} will have $2M$ nonzero singular values. Accordingly, U and V can be divided into $U = [U_s \ U_n]$ and $V = [V_s \ V_n]$, where U_s and V_s denote the first $2M$ columns of U and V respectively. From Eq. (8), it can be seen that the basis vectors of U_s and V_s are $\{\mathbf{g}_{1_\Re}^r, \cdots, \mathbf{g}_{M_\Re}^r, \mathbf{g}_{1_\Im}^r, \cdots, \mathbf{g}_{M_\Im}^r\}$ and $\{\mathbf{g}_{1_\Re}^t, \cdots, \mathbf{g}_{M_\Re}^t, \mathbf{g}_{1_\Im}^t, \cdots, \mathbf{g}_{M_\Im}^t\}$ respectively. Since U and V have orthogonal columns, $\mathbf{g}_m^r$ is orthogonal to the columns of U_n and $\mathbf{g}_m^t$ is orthogonal to columns of V_n, for all $m \in \{1, 2, \cdots, M\}$. For any arbitrary location $\mathbf{x}_p \in \mathbf{D}$, let $\mathbf{g}_p^r = [G(\mathbf{x}_1^r, \mathbf{x}_p), G(\mathbf{x}_2^r, \mathbf{x}_p), \cdots, G(\mathbf{x}_{N_r}^r, \mathbf{x}_p)]$ and $\mathbf{g}_p^t = [G(\mathbf{x}_1^t, \mathbf{x}_p), G(\mathbf{x}_2^t, \mathbf{x}_p), \cdots, G(\mathbf{x}_{N_t}^t, \mathbf{x}_p)]$. Following a similar procedure of [5], it can be shown that $\mathbf{g}_p^r$ is orthogonal to all the columns of U_n, and $\mathbf{g}_p^t$ is orthogonal to all the columns of V_n, if and only if $\mathbf{x}_p = \mathbf{x}_m$, for $m \in \{1, 2, ..., M\}$. Therefore, the image of the targets in the workspace, $I(\mathbf{x}_p)$, can be estimated from the pseudospectrum, $I_{\text{ps}}(\mathbf{x}_p)$, defined as follows:

$$I(\mathbf{x}_p) = I_{\text{ps}}(\mathbf{x}_p) \triangleq \frac{1}{A_R} \times \frac{1}{A_T}, \tag{9}$$

where A_R and A_T are the projections of $\mathbf{g}_p^r$ and $\mathbf{g}_p^t$ on U_n and V_n, respectively, and can be computed as $A_R = \frac{\mathbf{g}_p^{r\,H} U_n U_n^H \mathbf{g}_p^r}{\mathbf{g}_p^{r\,H} \mathbf{g}_p^r}$ and $A_T = \frac{\mathbf{g}_p^{t\,T} V_n V_n^H \mathbf{g}_p^{t\,*}}{\mathbf{g}_p^{t\,H} \mathbf{g}_p^t}$. It can be seen that $I(\mathbf{x}_p)$ peaks only at the locations of the targets, since the projections in the denominator of Eq. (9) vanish at the locations of the targets. Therefore, $I(\mathbf{x}_p)$ represents the image of the targets in $\mathbf{D}$.

Remark 1: Note that the minimum required number of antennas to enable the aforementioned analysis is $2M + 1$, which is considerably less than the state-of-the-art value of M^2+1. If one array is utilized for both Tx and Rx, this will be the minimum required number of transceivers. If, on the other hand, two arrays are utilized for transmission and reception, then each array has to have at least $2M + 1$ elements.

IV. Simulation Results

In this section, we evaluate our framework to image the targets in a workspace $\mathbf{D}$ using simulations. We consider a square workspace of dimensions 4 m $\times$ 4 m which contains M point targets with permittivity of $5\epsilon_0$. Multiple objects with permittivity of $3\epsilon_0$ are randomly distributed throughout the workspace to form the clutter. In order to image the targets, we first perform a calibration of the workspace in which wireless power measurements are obtained in the absence of the targets. More specifically, each Tx antenna illuminates $\mathbf{D}$, one at a time, while all the receivers measure the received power of the wireless signals, thus obtaining a matrix P^{cl}. When the targets are present in the workspace, we then repeat the measurement process to obtain the data matrix P. P^{tg} is then obtained by taking the difference between P and P^{cl}. This matrix is then used to image the targets as described in Section III. We next present our results.

A. Noise-free case - Single array

In this section, we consider a single antenna array which acts as both Tx and Rx, i.e., each antenna in the array transmits and receives the wireless signals, as shown in Fig. 1. We further neglect modeling errors, i.e., we assume that the wireless power measurements follow the Rytov model given in Eq. (3). We use $N_t = N_r = 11$ antennas, with antenna separation of λ, located on the northern side of the workspace to image $M = 4$ targets in the workspace. Fig. 2 (top) shows the magnitude of the singular values of the matrix P^{tg}. It can be seen that the number of nonzero singular values are $2M = 8$ corresponding to 4 targets. Fig. 2 (bottom) shows the imaging result. The crosses represent the true locations of the targets. The 2D color map shows the magnitude of the

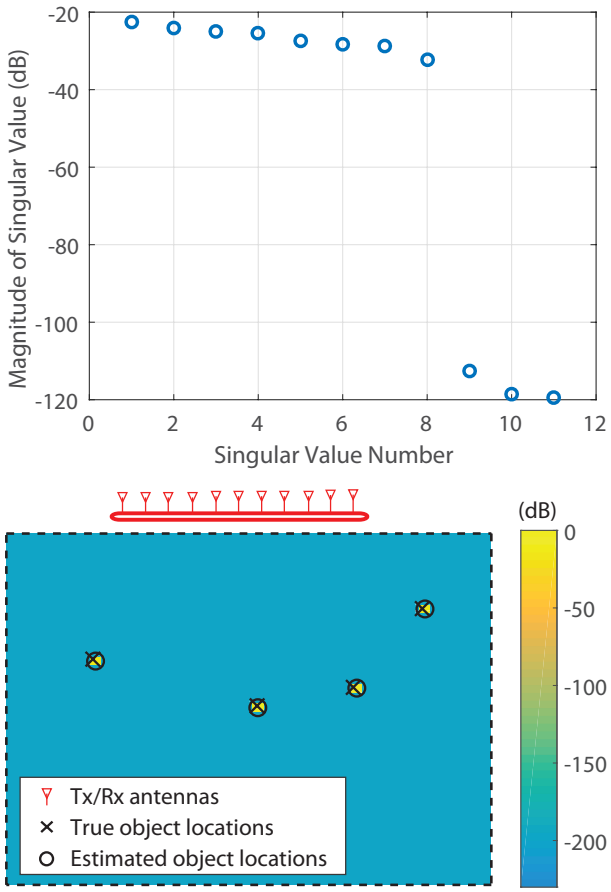

Fig. 2. (top) shows the magnitude of the singular values of the data matrix. It can be seen that the number of non-zero singular values are twice the number of the targets in the workspace. (bottom) shows the magnitude of the image of the targets in the workspace in dB. It can be seen that our framework accurately images the targets.

image I defined in Eq. (9). Then, the targets are estimated to be at the peaks (local maxima) of this 2D map, as indicated by circles in Fig. 2. It can be seen that, for the noiseless case, an accurate high-resolution image of the targets is obtained, which validates our framework.

B. Noisy case - Single array

To test the robustness of our framework to different types of errors, we consider modeling and measurement errors in this section. More specifically, the power measurements are obtained by solving the exact forward model of Eq. (1). Furthermore, we add an additive white Gaussian noise to the receptions ($P_{\mathbf{D}}$) such that the signal to noise ratio (SNR) of the power measurements is 40 dB. Same configuration of the antennas of the noise free case is used to image $M = 4$ targets. Fig. 3 shows the imaging result. As the figure shows, the target locations are accurately imaged even in the presence of modeling errors and noise.

C. Noisy case - Two arrays

In this section, we consider two different arrays for Tx and Rx antennas. Although using two separate arrays for Tx and

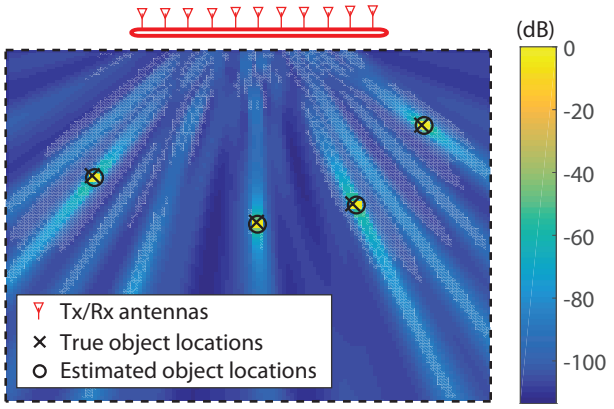

Fig. 3. Magnitude of the image, in dB, in the presence of modeling errors and noise. It can be seen that our framework accurately images the targets.

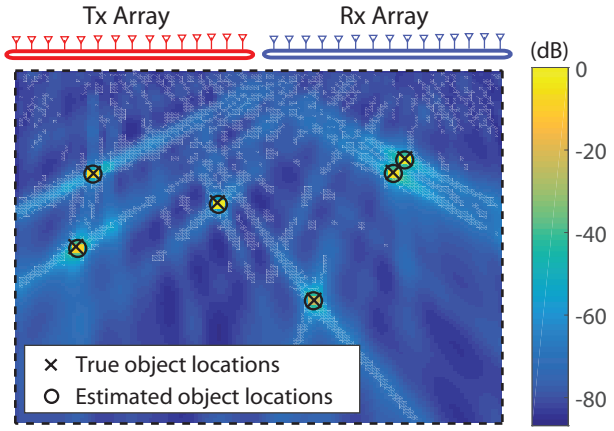

Fig. 4. Magnitude of the image, in dB, in the presence of modeling errors and noise when using two antenna arrays. It can be seen that our framework accurately images the targets.

Rx increases the total number of required wireless nodes, a higher resolution can be achieved compared to the single array case [10]. We position the two arrays on the same side of the workspace with their centers separated by 19λ. Each array consists of 16 antennas, i.e., $N_t = N_r = 16$, with antenna separation of λ. The workspace contains $M = 6$ targets, two of which are located only 2.5λ apart. Fig. 4 shows our imaging result. It can be seen that all the targets, including the closely-located ones, are imaged and resolved accurately.

V. Conclusion

In this paper, we presented an approach to reduce the number of Tx/Rx antennas for high-resolution imaging using only wireless power measurements. We modeled the received power of the array using Rytov wave model. We then showed that by spacing the antennas at the multiples of the wavelength and extending the existing TR-MUSIC algorithm, we can image M targets using only $2M + 1$ Tx/Rx antennas, a significant reduction from the state-of-the-art value of M^2+1. We finally validated our framework with simulation results.

REFERENCES

[1] S. Depatla, L. Buckland, and Y. Mostofi, "X-Ray vision with only WiFi power measurements using Rytov wave models," *IEEE Trans. on Vehicular Technology*, vol. 64, pp. 1376–1387, 2015.

[2] A. Gonzalez-Ruiz, A. Ghaffarkhah, and Y. Mostofi, "An integrated framework for obstacle mapping with see-through capabilities using laser and wireless channel measurements," *IEEE Sensors Journal*, vol. 14, no. 1, pp. 25–38, 2014.

[3] M.G.Amin, *Through-the-wall radar imaging*. CRC press, 2016.

[4] N. Joachimowicz, C. Pichot, and J. Hugonin, "Inverse scattering: An iterative numerical method for electromagnetic imaging," *IEEE Trans. on Antennas and Propagation*, vol. 39, no. 12, pp. 1742–1753, 1991.

[5] A. J. Devaney, "Super-resolution processing of multi-static data Using Time Reversal and MUSIC," *J. the Acoustical Society of America*, 2000.

[6] E. Marengo, R. Hernandez, and H. Lev-Ari, "Intensity-only signal-subspace-based imaging," *J. the Optical Society of America*, vol. 24, no. 11, pp. 3619–3635, 2007.

[7] Y. Zhuo, H. Zhu, and H. Xue, "Identifying a new non-linear CSI phase measurement error with commodity WiFi devices," in *IEEE 22nd International Conf. on Parallel and Distributed Systems (ICPADS)*, 2016.

[8] A. Novikov, M. Moscoso, and G. Papanicolaou, "Illumination strategies for intensity-Only imaging," *SIAM J. Imaging Sciences*, vol. 8, no. 3, pp. 1547–1573, 2015.

[9] W. Chew, *Waves and fields in inhomogeneous media*. IEEE Computer Society Press, 1995.

[10] S. K. Lehman and A. J. Devaney, "Transmission mode time-reversal super-resolution imaging," *J. the Acoustical Society of America*, vol. 113, no. 5, pp. 2742–2753, 2003.